City-wide Solar Radiation Potential Analysis by Coupling Physical Modelling and Machine Learning

Xiana Chen[1,2,3,4], Junxian Yu[2], Wei Tu[1,2,3,4], Long Chen[5]

1 Guangdong Key Laboratory of Urban Informatics, Shenzhen University, Shenzhen, Guangdong 518060, China - chenxiana2019@email.szu.edu.cn, 2019104015@email.szu.edu.cn, tuwei@szu.edu.cn
2 Ministry of Natural Resources Key Laboratory for Geo-Environmental Monitoring of Great Bay Area, Shenzhen University, Shenzhen, Guangdong 518060, China
3 Shenzhen Key Laboratory of Spatial Smart Sensing and Services, Shenzhen, Guangdong 518060, China
4 School of Architecture and Urban Planning, Shenzhen University, Shenzhen, Guangdong 518060, China
5 State Key Laboratory of Management and Control for Complex Systems, Institute of Automation, Chinese Academy of Sciences, Beijing, China - long.chen@ia.ac.cn

Keywords: Solar radiation potential, Machine learning, 3D buildings, Solar energy.

Abstract

Addressing the challenges posed by climate change and meeting urban energy demands is of utmost importance in today's world. Building Integrated Photovoltaics (BIPV) emerges as a crucial solution for energy conservation and carbon emissions reduction in urban environments. However, traditional methods of assessing solar radiation on buildings using physical models are often computationally intensive and time-consuming. This paper introduces a novel hybrid approach that integrates physical model-based solar radiation calculation with machine learning techniques to analyze Solar Radiation Potential (SRP) across city-wide building infrastructure. The proposed approach precisely evaluates the SRP of representative blocks by leveraging computing-intensive physical models integrated with 3D building data. Subsequently, two machine learning models are developed to effectively predict the SRP of building roofs and facades across the entire city. To validate the efficacy of this approach, an experiment was conducted in Shenzhen, China, yielding insightful results. The findings reveal that Shenzhen has a huge potential for BIPV solar power generation, with mean annual total building roof and facade solar radiation values of $9.22 * 10^7 kwh$ and $2.47 * 10^8 kwh$, respectively. It can be further observed that relying solely on rooftop installations is insufficient to meet electricity demand. This study not only provides an innovative alternative for city-wide SRP estimation by combining physical modeling and machine learning but also offers valuable insights for fostering low-carbon urban environments and informing data-driven and model-driven urban planning and management strategies.

1. Introduction

Global warming, energy shortages, and air pollution in cities have profound implications for human society. Consequently, humans have reached the consensus that reducing fuel-based energy consumption and carbon emissions and shifting to low-carbon sustainable development. Solar energy, which is characterized by low-cost, zero-pollution, and renew-ability, has become a necessity. For example, coupling with solar clean energy, electric vehicles can dramatically cut transportation emissions (Tu et al., 2019). Building Integrated Photovoltaic (BIPV) provides an alternative approach towards solar cities (Ji et al., 2024; Zhu et al., 2020). Quantifying city-wide solar radiation potential (SRP) is an essential task, given diverse building types and building distribution.

Traditional methods for estimating SRP on earth surfaces typically utilize ray tracing or sky models. These physically-based models take into account solar characteristics and atmospheric effects to provide accurate results. Various solar radiation tools have been developed for estimating building SRP. For instance, Peronato et al. (2018) utilized the Daysim tool to analyze solar radiation in a high-density urban area, showing promising results. It was shown that the absolute time for the simulation of the tile at a resolution of 0.5 m (over 16 hours) is great for large-scale applications. These tools significantly advance solar energy research but are computationally expensive for complex urban environments.

Recently, there has been a shift from traditional physical modelling to data-driven approaches to quantification (Cao et al., 2022), such as solar radiation from urban buildings (Vartholomaios, 2019). Walch et al. (2020) identified Random Forest (RF) as the most accurate among five popular Machine Learning (ML) models in predicting urban solar potential. Their study demonstrated the ability of ML-based SRP estimation. However, models trained with only tens of buildings exhibit poor generalization. They are not suitable for city-wide SRP estimation scenarios.

Light detection and ranging (LiDAR) and Oblique photogrammetry enable the acquisition of high-precision 3D urban models, enhancing the integration of digital and physical cities in planning and construction (Gruen, 2013). These models have been extensively utilized in urban energy simulation, facilitating highly accurate SRP analysis (Fang et al., 2021; Schrotter & Hürzeler, 2020). However, city-wide SRP calculations face practical challenges, especially the intensive-computing effort of physical models. How to couple 3D urban models, physical models, and ML for city-wide SRP should be further investigated.

To fill the above gaps, this study presents a hybrid methodology integrating 3D buildings, a physical model, and ML. We leverage a physical model for high-fidelity SRP computation on representative blocks. ML then efficiently estimates city-wide building SRP, balancing accuracy and efficiency. A city-wide experiment conducted in Shenzhen, China demonstrates the performance of the presented hybrid approach.

2. Study area and data

2.1 Study area

The research was carried out in Shenzhen, Guangdong Province, China, located at approximately N22°27' ~ 22°52', E113°46' ~ 114°37'. Shenzhen boasts a typical subtropical maritime monsoon climate, characterized by mild temperatures, ample rainfall, and extended sunshine. With an average of 1853 hours of sunshine annually, and it's noted that the daily average horizontal solar radiation peaks in July at around 4.96 kwh/m^2. These favorable natural conditions provide a robust basis for solar energy exploitation in Shenzhen. The city has set ambitious targets, aiming to achieve 10 million kilowatts of installed solar power capacity by 2025, with renewable energy accounting for 10% of its total energy consumption, as stated by the Shenzhen Municipal People’s Government.

2.2 Study data

To analyse city-wide SRP, three datasets were employed: 3D building data, comprehensive meteorological data, and road networks. The building dataset details the 3D information of 644,307 buildings, covering the whole Shenzhen. The meteorological dataset spans from 1980 to 2018, including information such as temperature, humidity, wind speed, direct radiation, and rainfall. It offers comprehensive meteorological information affecting Shenzhen’s solar radiation conditions. Additionally, road data was obtained using the Baidu Maps Open Platform API, including main roads, highways, and expressways. These road data underwent topological processing to ensure the integrity and accuracy of the road network.

3. Methodology

This study aims to assess and analyse the buildings’ SRP across the whole city by combining a physical model and ML with 3D urban models. It includes four main steps, as shown in Figure 1. Firstly, the whole city is divided into blocks using road network data. The morphology indicators for each block in terms of four aspects - height, area, volume and density - are calculated. Then, the buildings’ SRP of representative blocks is precisely calculated with the computing-intensive physical model. Thirdly, ML models are trained and the best models are selected to estimate the remained blocks. Finally, city-wide SRP is analysed based on the trained ML model. Details are described as follows.

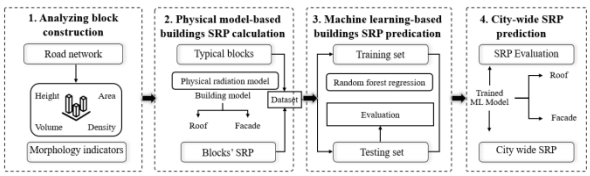

Figure 1. Overview of methodology.

3.1 Physical model-based buildings solar radiation potential calculation

Physical models account for various factors like direct sunlight, diffuse radiation, and ground reflection for accurate solar energy assessments. They employ standard atmospheric models, the Perez model (Perez et al., 1990) can be used to determine absorption coefficients and diffuse radiation components, and ray tracing algorithms to calculate building shading effects.

By combining the contributions from direct $Dir(x,y,z)$ and diffuse $DHI(x,y,z)$ radiation, the total solar radiation at each point (x, y, z) is calculated as Eq (1).

$$G(\mathrm{x},\mathrm{y},\mathrm{z}) = Dir(\mathrm{x},\mathrm{y},\mathrm{z}) + DHI(\mathrm{x},\mathrm{y},\mathrm{z}) \quad (1)$$

Direct solar radiation is computed as Eq (2). It considers atmospheric transmittance, absorption coefficients, building shading effects, and solar incidence angle.

$$Dir(x,y,z) = G_0 * K_T * K_a * F_{shadow}(x,y,z) * cos\,(\theta(x,y,z)) \quad (2)$$

where $Dir(x,y,z)$ = direct solar radiation
G_0 = top-of-atmosphere solar radiation
K_T = atmospheric transmittance coefficient
K_a = absorption coefficient
F_{shadow} = building shadow factor
θ = solar incidence angle

Diffuse radiation refers to sunlight that has been scattered by the atmosphere, clouds, and surfaces.

$$DHI(x,y,z) = DHI_{clear} * C_{diffuse} * C_{cloud} \cdot (1 - cos^3(Z(\mathrm{x},\mathrm{y},\mathrm{z}))) * F_{shadow}(\mathrm{x},\mathrm{y},\mathrm{z}) + G_{\mathrm{refl}}(\mathrm{x},\mathrm{y},\mathrm{z}) \quad (3)$$

where DHI_{clear} = clear sky diffuses
C_{diffuse} = atmospheric diffuse coefficient
C_{cloud} = cloud cover factor
Z = solar elevation angle
F_{shadow} = building shading factor
G_{refl} = ground reflection

Given the representation of the urban landscape in Shenzhen, blocks in Futian and Longhua district are selected for training. These districts represent the spectrum of urban landscapes, from high-rise commercial centers to mixed-use suburban areas, reflecting Shenzhen's rapid urbanization and socioeconomic diversity. Therefore, using these districts allows for capturing a broad range of urban morphologies and characteristics. The urban surface was discretized into 2m x 2m grids to obtain 6.25 million building roof points and 1.67 billion building facade points across 5613 buildings in 369 selected blocks. Solar radiation was calculated for each point considering weather data, surrounding structures, and 3D building, and finally be aggregated to the block level.

3.2 Machine learning-based buildings SRP estimation

Machine Learning (ML) is employed to capture the non-linear relationship between the morphological indicators of urban blocks and their overall SRP values as calculated by a physical model. Specifically, four features of building form—height, area, volume, and density—are considered. Fourteen indicators are selected to quantitatively characterize each urban block, serving as the independent variable x. The details of these indicators are provided in Table 1. The total annual solar radiation values for all discrete points on building roofs and facades within a block are aggregated to form the dependent variable y in two separate models. Several typical ML models, including K-Nearest Neighbour, Support Vector Regression, Decision Tree, and Random Forest (RF), are trained. By comparing their accuracies, we determined that the RF model is the most effective for further training. This approach aims to estimate the overall SRP value of a block based

on its comprehensive morphological indicators, rather than linking each SRP grid point directly to its morphological indicators.

Group	Variables	Calculating expression
Height	Total Height	$\sum_{i=1}^{n} h_i$
	Average Height	$\frac{1}{n}\sum_{i=1}^{n} h_i$
	Height Standard Deviation	$\sqrt{\frac{\sum_{i=1}^{n}(h_i - \mathrm{AVH})^2}{n}}$
Area	Total Building Roof Area	$\sum_{i=1}^{n} s_i$
	Total Surface Area	$\mathrm{TBRA} + \sum_{i=1}^{n} h_{li} * l_{li}$
	Roof Area Ratio	$\frac{\mathrm{TBRA}}{\mathrm{TSA}}$
Volume	Total Volume	$\sum_{i=1}^{n} h_i * s_i$
	Average Volume	$\frac{1}{n}\sum_{i=1}^{n} h_i * s_i$
	Surface Area Density	$\frac{\mathrm{TSA}}{\mathrm{TVV}}$
Density	Building Surface Fraction	$\frac{\sum_{i=1}^{n} s_i}{S_{total}}$
	Building Count Density	$\frac{n}{S_{total}}$
	Floor Area Ratio	$\frac{\mathrm{TFA}}{S_{total}}$
	Aspect ratio	$W = \frac{\sum_{k=1}^{C_n^2} NA_k(B_i, B_j)}{C_n^2}$ $\frac{\mathrm{AVH}}{W}$
	Sky View Factor	$\Omega = 2\pi\left[1 - \frac{\sum_{i=1}^{m} \sin\gamma_j}{m}\right]$ $svf_j = 1 - \frac{\sum_{i=1}^{m} \sin\gamma_j}{m}\frac{1}{k}\sum_{j=1}^{k} svf_j$

Table 1. Urban morphology indicators for machine learning-based building solar radiation potential calculation.

Note: n represents the number of buildings in the Local Climate Zone, S_{total} represents the total area of the block, h_i denotes the height of building i, s_i indicates the footprint area of building i, l_i signifies the perimeter of building i, and f_i stands for the number of floors in building i.

The data (Urban morphology in Table 1 and physical model SRP at a block level) was standardized and split for training (80%) and testing (20%). The model was trained on standardized data split 8:2 for training and testing. Hyperparameters were tuned using 10-fold cross-validation to optimize the final ML model. The coefficient of determination (R^2) and the Mean Absolute Percentage Error (MAPE) were used to assess the model performance.

Finally, the trained ML model is used to predicate the SRP of building roofs and facades across the whole city. The obtained annual SRP can then be mapped city-wide. It facilitates the evaluation of renewable energy potential across different blocks and the associate carbon emission benefits.

4. Results and Analysis

4.1 Results of physical model-based solar radiation potentials

The SRP of 369 blocks in Futian and Longhua districts were calculated with a physical solar radiation model. The computation time of one block was approximately 10 minutes on a computer with an Intel Core i7-10750H processor and 16 GB of RAM. Consequently, evaluating the SRP for all 1671 blocks in Shenzhen would require around 15 days, which is impractical for timely decision-making.

Figure 2 illustrates the building solar radiation in Futian District. Panel (a) presents the 3D building data of Futian, while panels (b) and (c) display the simulation results of solar radiation on the roofs and facades of buildings in selected blocks, respectively. Similarly, Figure 3 depicts the building solar radiation in Longhua District. Panel (a) shows the 3D building data of Longhua, with panels (b) and (c) illustrating the simulation results of solar radiation on the roofs and facades of buildings in certain blocks, respectively. Overall, blocks with significant SRP on their roofs also have substantial SRP potential on their facades. However, the total SRP of roofs is rarely greater than that of facades.

In statistical terms, the average SRP values for building roofs in Futian and Longhua districts are around 8.61×10^7kwh and 8.38×10^7 kwh, respectively. Likewise, the average annual SRP values for building facades in Futian and Longhua are approximately 1.48×10^8kwh and 9.20×10^7kwh, respectively. When considering both roofs and facades together, the total SRP is approximately 2.34×10^8kwh for Futian, slightly exceeding Longhua District's total of 1.76×10^8kwh.

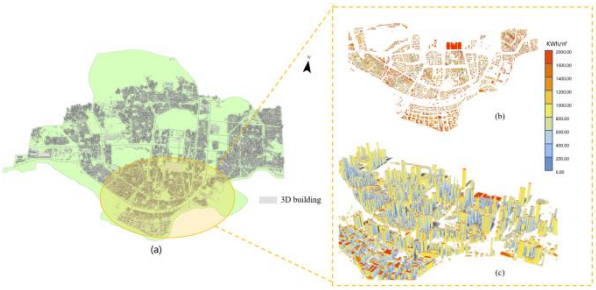

Figure 2. Building solar radiation in Futian District. (a) 3D building data of Futian, (b) Simulation results of solar radiation on roofs of buildings in some blocks, (c) Simulation results of solar radiation on facades of buildings in some blocks.

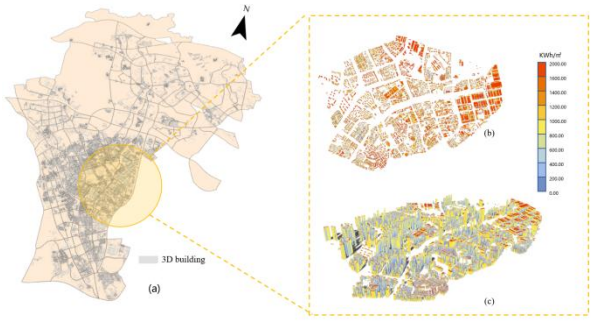

Figure 3. Building solar radiation in Longhua District. (a) 3D building data of Longhua, (b) Simulation results of solar radiation on roofs of buildings in some blocks, (c) Simulation results of solar radiation on facades of buildings in some blocks.

4.2 Results of city-wide solar radiation potential

For building roof SRP, the trained RF achieved an R^2 of 0.80 on the test set (MAPE: 0.06) and 0.85 on cross-validation (MAPE: 0.18). For building facade SRP, the RF yielded an R^2 of 0.75 on the test set (MAPE: 0.13) and 0.70 on cross-validation (MAPE: 0.21). These models demonstrated strong performance and are suitable for estimating city-wide building SRP.

Using the trained model for calculating the total solar radiation potential of building roofs, the total value of solar radiation from building roofs within the city of Shenzhen was calculated. Figures 4 and 5 reflect the spatial distribution of the size and statistics of the solar radiation received by building roofs in different blocks, respectively. As can be seen from the figures, building roofs in most areas of Shenzhen have a high solar radiation potential, with an average value of $9.22 * 10^7 kwh$. The total solar radiation potential of building roofs in Yantian, Bao'an, Pingshan, and Longgang districts is at a higher level, and the total solar radiation potential of building roofs in most of the local climatic zones is higher than that of the whole city. total rooftop solar radiation potential is higher than the citywide average, while Nanshan, Futian and Luohu districts are relatively low.

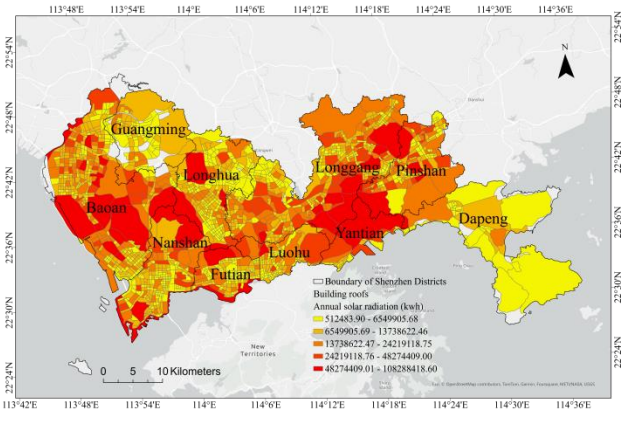

Figure 4. Spatial distribution of building roof SRP in Shenzhen.

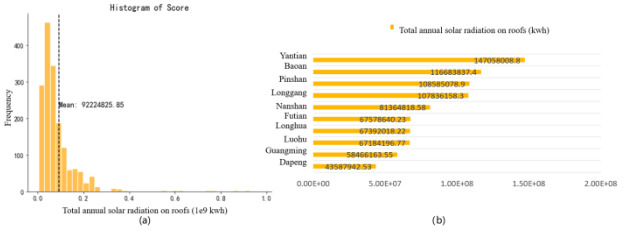

Figure 5. Statistical analysis of building roof solar potential by districts in Shenzhen. (a) Histogram of annual solar radiation potential of roofs in block scale. (b) District comparison of mean annual solar radiation potential of roofs in blocks.

Using the model for calculating the total solar radiation potential of building facades, the total solar radiation value of building facades within the city of Shenzhen was calculated, and Figures 6 and 7 reflect the spatial distribution of the magnitude and statistics of the solar radiation received by building facades across the city, respectively. From the figures, it can be seen that building facades in most areas of Shenzhen have high solar radiation potential, with an average value of $2.47 * 10^8 kwh$. The total solar radiation potential of building facades in Guangming and Dapeng New Districts is lower, and the total solar radiation potential of building facades in most of the blocks is lower than the citywide average level.

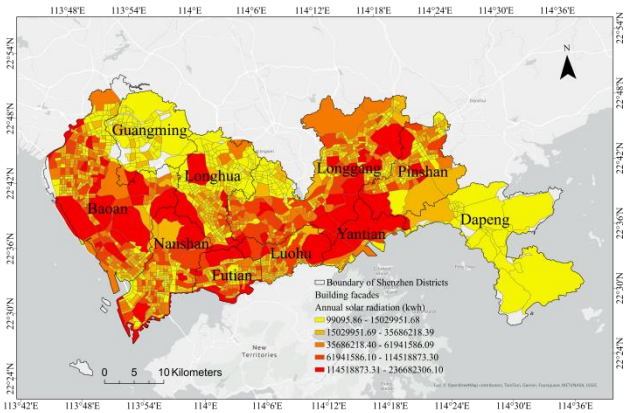

Figure 6. Spatial distribution of building facade SRP in Shenzhen.

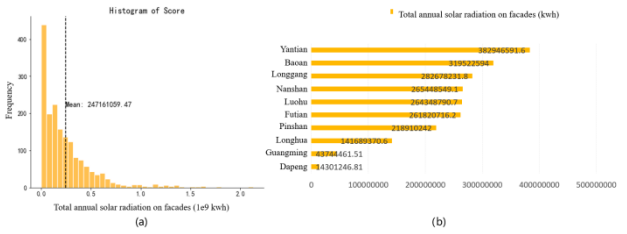

Figure 7. Statistical analysis of building facade SRP by districts in Shenzhen. (a) Histogram of annual solar radiation potential of roofs in block scale. (b) District comparison of mean annual solar radiation potential of facades in blocks.

5. Discussion

5.1 Advancing Solar Potential Assessment through Integrated Physical Models and Machine Learning

This study represents a significant advancement in solar potential

assessment by harnessing the synergies between physical models and ML algorithms. Physical models excel in accurately simulating solar illumination within urban environments, providing precise insights into SRP. However, the computational demands of these models can be prohibitive, particularly when applied to large and complex datasets encompassing entire cities. In contrast, ML techniques offer a rapid and efficient means of assessing SRP for city-wide buildings, enabling expedited decision-making processes for urban planners, architects, and governmental agencies. By integrating physical and ML models, this approach capitalizes on the strengths of each method, ensuring both accuracy and speed in city-wide SRP analysis. This integration not only enhances the efficiency of urban planning processes but also enables more informed decision-making regarding solar energy utilization and infrastructure development.

Moreover, the combination of physical and ML models addresses the challenge of incomplete data coverage in urban contexts. Physical models typically require high-precision input data, which may be challenging to obtain in areas with limited architectural details. ML algorithms offer a solution by partially compensating for data gaps, allowing for SRP calculations even in regions with incomplete data coverage. In this study, ML models were trained using simulated solar radiation results from existing 3D buildings, enabling assessments in areas where data was previously unavailable.

Furthermore, the hybrid approach demonstrated in this study suggests the potential for model generalization, implying that similar methods could be effectively applied to analogous urban settings. This not only simplifies the assessment of solar potential in diverse urban contexts but also enhances the scalability and applicability of solar energy planning strategies.

5.2 Analysis of the rate of satisfaction of electricity demand in buildings

To evaluate the photovoltaic power supply rate in Shenzhen, this study calculated the electricity consumption in various blocks of the city. The 2019 electricity consumption data used in this study was collected from Chen et al.'s research (2022), which calculated the actual GDP and electricity consumption within a global one-kilometer grid based on calibrated nighttime light data from 1992 to 2019. The data can be accessed at https://doi.org/10.6084/m9.figshare.17004523.v1. This study assumes a 20% conversion rate of solar energy to electricity for photovoltaic equipment. The electricity supply rate is represented by the ratio of the total solar radiation potential on building surfaces to the electricity demand.

Figures 8 and 9 show the distribution of electricity demand satisfaction when photovoltaic equipment is installed only on rooftops and facades, respectively. It can be observed that relying solely on rooftop installations is insufficient to meet electricity demand. Installing photovoltaic equipment on building facades can significantly improve the electricity supply rate. Promoting the use of building facades for photovoltaics can effectively enhance the utilization of renewable energy. In Dapeng New District and Guangming District, the supply rate is relatively low. Therefore, other sustainable energy generation methods, such as wind power, should be considered.

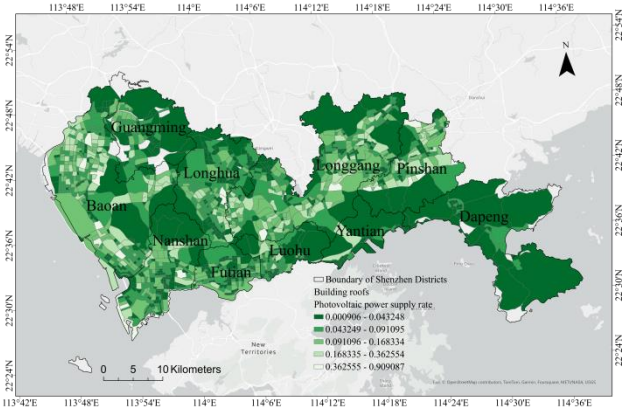

Figure 8. Distribution of electricity demand satisfaction with photovoltaic equipment installed only on rooftops.

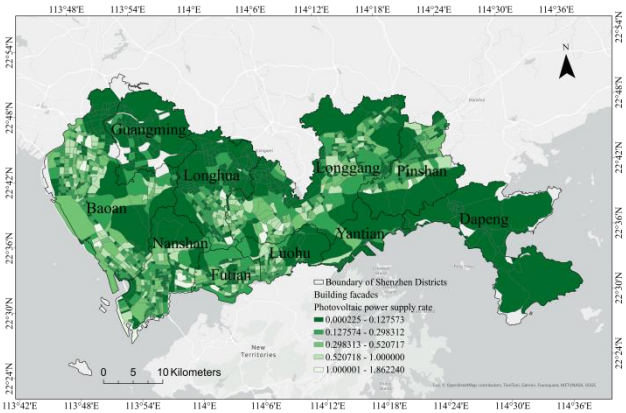

Figure 9. Distribution of electricity demand satisfaction with photovoltaic equipment installed only on facades.

5.3 Limitation and future work

While this study had made strides in analyzing urban building SRP, limitations persist. Though our study has made significant progress in analyzing urban building SRP, we only considered building morphological indicator based on the available data. Incorporating finer details, including information on building and road materials, could enhance the accuracy and applicability of the model. The inclusion of building and road material data can provide valuable insights into the interaction between surface properties and solar radiation absorption, thereby enriching our understanding of SRP distribution within urban areas. Furthermore, there is an opportunity to enhance the adaptability of the ML model across diverse environmental conditions. Expanding the dataset to include a broader range of climate and geographic regions would improve the model's robustness and generalizability, facilitating more accurate predictions of SRP in various urban contexts. By addressing these limitations and incorporating finer data resolution, we aim to advance our understanding of urban SRP dynamics and contribute to more effective strategies for sustainable urban development.

6. Conclusion

This study offers a novel hybrid method combining physical models and machine learning for efficient, city-wide building SRP analysis. The results of the study in Shenzhen, China, show that Shenzhen has a huge potential for BIPV solar power generation, with mean annual total building roof and facade solar radiation values of $9.22 * 10^7 kwh$ and $2.47 * 10^8 kwh$, respectively.

In conclusion, this study has made several significant contributions to the field of urban solar energy potential assessment and sustainable urban development. Firstly, by presenting a hybrid approach that integrates physical models with ML, we have achieved both accuracy and scalability in SRP mapping. This innovative methodology not only confirms the research paradigms of GeoAI but also lays the groundwork for quantitative studies of various complex geographic phenomena, extending its applicability to diverse urban contexts.

Secondly, our comprehensive city-wide assessment of SRP has provided valuable insights into the solar energy potential of urban areas. By shedding light on the SRP distribution across different building configurations, this research serves as a catalyst for cities to explore green building practices and adopt sustainable development strategies. This holistic understanding of urban solar energy dynamics is essential for fostering a more sustainable urban future.

Future research efforts can focus on enhancing simulation accuracy by incorporating detailed 3D model data and employing more accurate ML models. By addressing these aspects, future research endeavors can further advance the scientific basis for urban planning and management, ultimately promoting sustainable urban development on a global scale.

Acknowledgements

This study is supported and funded by the National Natural Science Foundation of China (No. 42071360, 42311530335, 42101472); The Key Project of Shenzhen Commission of Science and Technology (No.JCYJ20220818100200001); Science and technology program of Ningbo, China (2023S171).

References

Cao, R., Tu, W., Cai, J., Zhao, T., Xiao, J., Cao, J., Gao, Q., Su, H., 2022. MACHINE LEARNING-BASED ECONOMIC DEVELOPMENT MAPPING FROM MULTI-SOURCE OPEN GEOSPATIAL DATA. *ISPRS Annals of the Photogrammetry, Remote Sensing and Spatial Information Sciences*, V-4–2022, 259–266. doi.org/10.5194/isprs-annals-V-4-2022-259-2022.

Chen, J., Gao, M., Cheng, S., Hou, W., Song, M., Liu, X., Liu, Y., 2022. Global 1 km × 1 km gridded revised real gross domestic product and electricity consumption during 1992–2019 based on calibrated nighttime light data. *Scientific Data*, 9(1), Article 1. doi.org/10.1038/s41597-022-01322-5.

Fang, Z., Shaw, S.-L., Yang, B., Santi, P., Tu, W., 2021. Integrated environmental and human observations for smart cities. *Environment and Planning B: Urban Analytics and City Science*, 48(6), 1375–1379. doi.org/10.1177/23998083211023296.

Gruen, A., 2013. SMART Cities: The need for spatial intelligence. *Geo-Spatial Information Science*, 16(1), 3–6. doi.org/10.1080/10095020.2013.772802.

Ji, N., Zhu, R., Huang, Z., You, L., 2024. An urban-scale spatiotemporal optimization of rooftop photovoltaic charging of electric vehicles. *Urban Informatics*, 3(1), 4. doi.org/10.1007/s44212-023-00031-7.

Peronato, G., Rey, E., Andersen, M., 2018. 3D model discretization in assessing urban solar potential: The effect of grid spacing on predicted solar irradiation. *Solar Energy*, 176, 334–349. doi.org/10.1016/j.solener.2018.10.011.

Schrotter, G., Hürzeler, C., 2020. The Digital Twin of the City of Zurich for Urban Planning. *PFG – Journal of Photogrammetry, Remote Sensing and Geoinformation Science*, 88(1), 99–112. doi.org/10.1007/s41064-020-00092-2.

Tu, W., Santi, P., Zhao, T., He, X., Li, Q., Dong, L., Wallington, T. J., Ratti, C., 2019. Acceptability, energy consumption, and costs of electric vehicle for ride-hailing drivers in Beijing. *Applied Energy*, 250, 147–160. doi.org/10.1016/j.apenergy.2019.04.157.

Vartholomaios, A., 2019. A machine learning approach to modelling solar irradiation of urban and terrain 3D models. *Computers, Environment and Urban Systems*, 78, 101387. doi.org/10.1016/j.compenvurbsys.2019.101387.

Walch, A., Castello, R., Mohajeri, N., Scartezzini, J.-L, 2020: A fast machine learning model for large-scale estimation of annual solar irradiation on rooftops. *Proceedings of Solar World Congress 2019*.

Zhu, R., Wong, M. S., You, L., Santi, P., Nichol, J., Ho, H. C., Lu, L., Ratti, C., 2020. The effect of urban morphology on the solar capacity of three-dimensional cities. *Renewable Energy*, 153, 1111–1126. doi.org/10.1016/j.renene.2020.02.050.